Check for updates

PODCAST 5-in-5

Indirect Head of the Rectus Femoris Tendon as a Graft for Segmental Hip Labral Reconstruction

An Anatomic, Radiographical, and Biomechanical Study in Comparison With Iliotibial Labral Reconstruction

Safa Gursoy,* MD, PhD, Felipe Bessa,† MD, Navya Dandu,† MD, Zeeshan A. Khan,‡ BA, Hailey P. Huddleston,† MD, Brady T. Williams,† MD, Amar S. Vadhera,† BS, Ian M. Clapp,† MD, Philip Malloy,† PT, PhD, Elizabeth F. Shewman,† MS, Shane J. Nho,† MD, and Jorge Chahla,†§ MD, PhD
Investigation performed at Rush University Medical Center, Chicago, Illinois, USA

Background: The indirect head of the rectus femoris (IHRF) tendon has been used as an autograft for segmental labral reconstruction. However, the biomechanical properties and anatomic characteristics of the IHRF, as they relate to surgical applications, have yet to be investigated.

Purpose: To (1) quantitatively and qualitatively describe the anatomy of IHRF and its relationship with surrounding arthroscopically relevant landmarks; (2) detail radiographic findings pertinent to IHRF; (3) biomechanically assess segmental labral reconstruction with IHRF, including restoration of the suction seal and contact pressures in comparison with iliotibial band (ITB) reconstruction; and (4) assess potential donor-site morbidity caused by graft harvesting.

Study Design: Descriptive laboratory study.

Methods: A cadaveric study was performed using 8 fresh-frozen human cadaveric full pelvises and 7 hemipelvises. Three-dimensional anatomic measurements were collected using a 3-dimensional coordinate digitizer. Radiographic analysis was accomplished by securing radiopaque markers of different sizes to the evaluated anatomic structures of the assigned hip. Suction seal and contact pressure testing were performed over 3 trials on 6 pelvises under 4 different testing conditions for each specimen: intact, labral tear, segmental labral reconstruction with ITB, and segmental labral reconstruction with IHRF. After IHRF tendon harvest, each full pelvis had both the intact and contralateral hip tested under tension along its anatomic direction to assess potential site morbidity, such as tendon failure or bony avulsion.

Results: The centroid and posterior apex of the indirect rectus femoris attachment are respectively located 10.3 ± 2.6 mm and 21.0 ± 6.5 mm posteriorly, 2.5 ± 7.8 mm and 0.7 ± 8.0 mm superiorly, and 5.0 ± 2.8 mm and 22.2 ± 4.4 mm laterally to the 12:30 labral position. Radiographically, the mean distance of the IHRF to the following landmarks was determined as follows: anterior inferior iliac spine (8.8 ± 2.5 mm), direct head of the rectus femoris (8.0 ± 3.9 mm), 12-o'clock labral position (14.1 ± 2.8 mm), and 3-o'clock labral position (36.5 ± 4.4 mm). During suction seal testing, both the ITB and the IHRF reconstruction groups had significantly lower peak loads and lower energy to peak loads compared with both intact and tear groups ($P = .01$ to .02 for all comparisons). There were no significant differences between the reconstruction groups for peak loads, energy, and displacement at peak load. In 60° of flexion, there were no differences in normalized contact pressure and contact area between ITB or IHRF reconstruction groups ($P > .99$). There were no significant differences between intact and harvested specimen groups in donor-site morbidity testing.

Conclusion: The IHRF tendon is within close anatomic proximity to arthroscopic acetabular landmarks. In the cadaveric model, harvesting of the IHRF tendon as an autograft does not lead to significant donor-site morbidity in the remaining tendon. Segmental labral reconstruction performed with the IHRF tendon exhibits similar biomechanical outcomes compared with that performed with ITB.

The American Journal of Sports Medicine
2024;52(7):1753–1764
DOI: 10.1177/03635465241251824
© 2024 The Author(s)

Clinical Relevance: This study demonstrates the viability of segmental labral reconstruction with an IHRF tendon and provides a detailed anatomic description of the tendon in the context of an arthroscopic labral reconstruction. Clinicians can use this information during the selection of a graft and as a guide during an arthroscopic graft harvest.

Keywords: hip arthroscopy; hip labrum; labral reconstruction; suction seal; biomechanics

Acetabular labral tears are one of the main causes of hip pain and disability in the young population[2,24] and are a common indication for hip arthroscopy.[34] The labrum deepens the acetabulum, thereby increasing the contact area of the hip joint, increasing hip stability, and forming a hydraulic suction seal.[38,41] This seal plays a vital role in hip kinematics, function, stability, and intra-articular fluid dynamics.[38,41] It is also hypothesized that the suction seal protects the cartilage matrix from load and decreases friction between the femoral head and acetabular surfaces.[2,10,29,31] In vitro investigations have reported that a partial labral resection results in an approximately 50% decrease in fluid pressurization while a complete resection may result in a reduction of >75% when compared with an intact condition.[10,31] Additionally, another biomechanical study demonstrated that the labrum serves as the main stabilizer for initial distractive forces, and in conditions of a simulated partial or complete tear, investigators observed significant reductions in distractive forces along with significant improvements after repair or reconstruction of the labrum.[29] When comparing patients who underwent labral debridement and refixation, Larson et al[16] found that >90% of those in the repair group had good to excellent outcomes versus only 68% in the debridement group after a mean follow-up of 3.5 years. Domb et al[8] similarly reported significantly better patient-reported outcomes for those with a labral reconstruction as compared with an excision.

Despite the existence of strong cohort-based evidence to support reconstruction over excision for the treatment of a nonsalvageable labrum, there is much debate in the literature regarding the best graft source for the reconstruction. Studies have reported good results with the use of autografts, such as the iliotibial band (ITB), indirect head of the rectus femoris (IHRF), gracilis, and semitendinosus tendons, as well as allografts, including semitendinosus and anterior tibialis tendons and fascia lata tissue.[‖] Comparatively, however, autografts are not predisposed to the risk of disease transmission and delayed incorporation[3] that is observed in allografts,[4] and local tissue autografts in particular minimize donor-site morbidity, eliminate the need for additional graft preparation, and preserve the distal blood supply of the grafted tissue.[1,20,33] In particular, the IHRF tendon has been cited as a suitable local graft for labral reconstruction for moderately sized tears, with excellent objective and patient-reported outcomes in small case series.[1,20,33] However, there is limited basic science literature regarding the IHRF tendon graft's capability to re-create the lost suction seal and contact pressure distribution. As such, the tendon biomechanical properties as well as its local anatomic and radiographic landmarks in the context of an arthroscopic reconstruction still need to be thoroughly investigated.

Therefore, the purpose of this study was to (1) quantitatively and qualitatively describe the anatomy of the IHRF and its relationship with surrounding arthroscopically relevant structures; (2) describe radiographic imaging of the IHRF and surrounding bony landmarks in addition to pertinent findings regarding tendon harvesting for an arthroscopic labral reconstruction; (3) assess potential donor-site morbidity caused by graft harvesting, including the increased risk for tendon rupture or avulsion; and (4) biomechanically assess the restoration of the suction seal and contact pressures within the hip joint after labral reconstruction with the IHRF graft. We hypothesized that the IHRF tendon would be in close proximity to the 12- to 3-o'clock labral positions and that harvest of an IHRF autograft would not reduce the biomechanical properties of the rectus femoris tendon. Additionally, we hypothesized that segmental labral reconstruction with IHRF autograft would have noninferior biomechanical properties compared with ITB, including contact area, contact pressure, peak force, peak distraction, cyclic creep, cyclic load, and maximal failure load.

METHODS

Specimen Selection and Preparation

Because of the use of deidentified specimens, this study was exempt from institutional review board approval.

[‖]References 1, 7, 18, 20, 22, 25, 27, 33, 43.

[§]Address correspondence to Jorge Chahla, MD, PhD, Department of Orthopaedic Surgery, Rush University Medical Center, 1611 W Harrison Street, Suite 300, Chicago, IL 60612, USA (email: jorge.chahla@rushortho.com).

*Department of Orthopaedic Surgery, Faculty of Medicine, Acibadem University, Istanbul, Turkey.

[†]Department of Orthopaedic Surgery, Rush University Medical Center, Chicago, Illinois, USA.

[‡]Rush Medical College, Chicago, Illinois, USA.

Submitted June 5, 2022; accepted February 6, 2024.

One or more of the authors has declared the following potential conflict of interest or source of funding: Stryker donated the suture anchors used in the study. S.J.N. has received research support from AlloSource, Arthrex, Athletico, DJ Orthopedics, Linvatec, Miomed, Smith & Nephew, and Stryker; consulting fees from Stryker; and royalties from Ossur and Stryker. J.C. has received consulting fees from Arthrex, CONMED Linvatec, Ossur, Smith & Nephew, DePuy Synthes Products, and Vericel; support for education from Medwest Associates; and hospitality payments from Medical Device Business Services and Stryker. AOSSM checks author disclosures against the Open Payments Database (OPD). AOSSM has not conducted an independent investigation on the OPD and disclaims any liability or responsibility relating thereto.

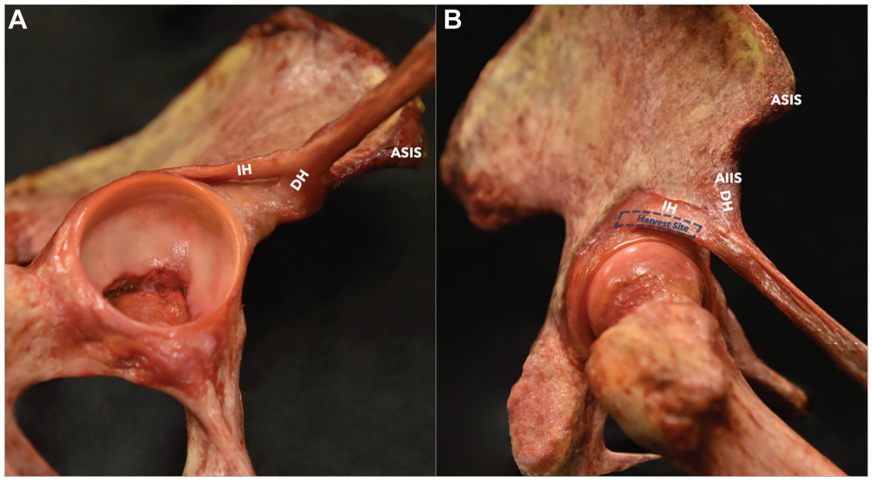

Figure 1. Cadaveric dissection photos of the rectus femoris muscle. (A) Anterior inferior view of the elevated indirect and direct heads of the rectus femoris muscle. (B) Demonstration of the indirect head of the rectus femoris tendon harvest site (blue dots) from a lateral-inferior view. AIIS, anterior inferior iliac spine; ASIS, anterior superior iliac spine; DH, direct head of the rectus femoris; IH, indirect head of the rectus femoris.

The cadaveric specimens were donated to a tissue bank for the purpose of medical research and then purchased by our institution. Eight fresh-frozen human cadaveric full pelvises (mean age, 54.9 years [range, 30-70 years]; mean body mass index, 26.1 [range, 19-33.4]) and 7 human cadaveric hemipelvises (mean age, 56.8 years [range, 36-68 years]; mean body mass index, 22.8 [range, 18.6-31.7]), without a history of osteoarthritis, local injury, or surgical intervention, were used. Specimens were delivered frozen and thawed at room temperature 48 hours before dissection. After thawing, the specimens were carefully dissected in an outside-in fashion. Any skin, subcutaneous tissue, and thigh or pericapsular muscles were removed, with meticulous dissection being performed to preserve the capsule and rectus femoris muscle. Before the investigation, hips within full pelvis specimens were randomized to be either anatomically and radiographically assessed or biomechanically tested. The additional 7 hemipelvises were only used for anatomic caliper measurements.

Anatomic Description

Anatomic data were collected using a combination of both digital calipers and a 3-dimensional (3D) coordinate digitizer (Microscribe; Solution Technologies) to project all structures in a 3D coordinate system (Rhinoceros 3D 5.0 software; McNeel North America). Using the digital calipers, we quantitatively described both the direct head of the rectus femoris and IHRF muscle along the course of each respective tendon (Figure 1), including length as well as both the width and the thickness at the proximal, midpoint, and distal aspects on 15 hemipelvises. Measurements were made by 2 independent investigators (S.G. and F.B.), and the mean of the 2 measurements was reported.

The IHRF and direct head of the rectus femoris were then carefully detached from bone on the 8 randomized hemipelvises and marked at their footprint areas and centers using a surgical marking pen for subsequent 3D coordinate measurement analysis, followed by the labrum in a similar fashion. On the acetabulum, the continuation of the stellate crease, the center of the psoas-U, and the midpoint of the transverse acetabular ligament (corresponding to the 12:30, 3:30, and 6-o'clock positions, respectively) were annotated using the 3D coordinate measuring device as previously described.[30]

During 3D coordinate data collection, each full pelvic specimen was rigidly secured to a baseplate. Using a custom fixture, we drilled 3 pins from lateral to medial through the ilium, with additional fixation being achieved using vice grips to ensure the stability of the specimen during data collection in a local coordinate frame block, thereby establishing the local anatomic axis. For full pelvic specimens, a local anatomic coordinate frame was established in accordance with previously established recommendations from the International Society of Biomechanics.[44] Specifically, the anteroposterior axis was established as a line perpendicular to and bisecting the lines connecting the 2 anterior superior and posterior superior iliac spines. The mediolateral axis was established parallel to the anterior superior and posterior superior iliac spine lines, while the inferosuperior axis was established as a line mutually perpendicular to the anteroposterior and mediolateral axes. Three-dimensional measurements were reported as absolute distances. Component measurements of the established anatomic axes were recorded when possible (full pelvic specimens) (Figure 2). To calculate anatomic distances (in mm) within the established Cartesian coordinate system, we used the Euclidean distance formula for the 3D plane [$d = \sqrt{(X_2 - X_1)^2 + (Y_2 - Y_1)^2 + (Z_2 - Z_1)^2}$] and 2-dimensional plane [$d = \sqrt{(X_2 - X_1)^2 + (Y_2 - Y_1)^2}$], respectively.

Radiographic Analysis

The radiographic analysis was accomplished by gluing radiopaque markers (metallic BBs) of different sizes to

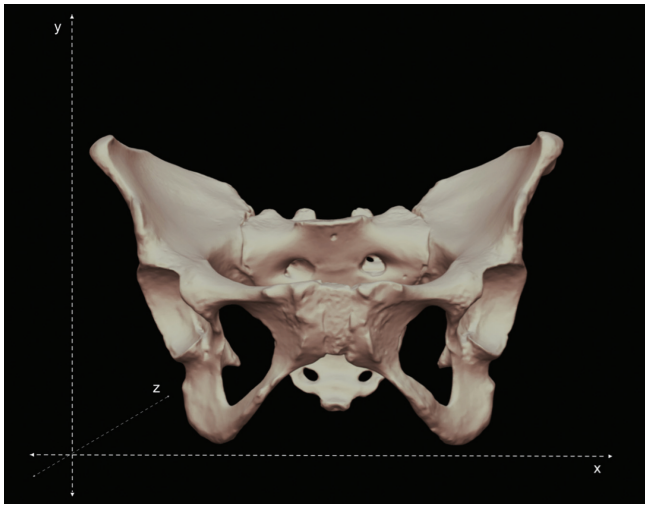

Figure 2. Representation of established *X*, *Y*, and *Z* planes relative to the pelvis for 3-dimensional coordinate system creation.

the assigned hips of each full pelvis at the center of the anterior inferior iliac spine, the center of both the direct head of the rectus femoris and IHRF tendons, and on the 12- and 3-o'clock positions of the acetabular rim (Table 1). The full bony pelvises were kept intact to allow for assessment of obliquity and rotation of the hips. An anteroposterior radiograph of the pelvis was obtained with the x-ray tube positioned 40 inches (101.6 centimeters) from the film. Digital images were visualized using a picture archiving and communication system (Viztek Opal-RAD; Konica Minolta).

Biomechanical Assessment

Suction seal effects and hip joint pressures were first assessed on the side of the full pelvises assigned randomly to biomechanical testing. The full pelvises were cut into 2 hemipelvises posteriorly from the median sacral crest and anteriorly from the pubic symphysis with the use of an oscillating saw, to allow for mounting the hips in a tensile testing system (Insight 5; MTS Systems Corp). The capsule was removed, the femur was distracted from the acetabulum, and the ligamentum teres was sectioned to disarticulate the hip. The hemipelvises were potted using dental acrylic (Isocryl; Lang Dental Manufacturing Co) to secure a portion of the ilium with the test equipment in a custom jig. The femur was also cut with an oscillating saw, preserving the proximal third of its diaphysis, which was potted axially in a cylindrical polyvinylchloride mold. The potted femur was fixed to the test machine base in a custom jig that allowed for angular positioning in 10° increments. For all 8 hip specimens, there were 4 different testing conditions for each specimen: (1) intact, (2) labral tear, (3) segmental labral reconstruction with the ITB, and (4) segmental labral reconstruction with the IHRF, with the 2 reconstruction methods performed in a random order. Suction seal, contact pressure, and donor-site morbidity testing were performed on each of the 8 hemipelvises.

TABLE 1
Sizes of the Radiopaque Markers and Correspondent Anatomic Structure

Radiopaque Marker	Anatomic Structure
1.5 mm	Direct head of the rectus femoris tendon center
2.0 mm	3 o'clock on acetabular rim
2.0 mm	Anterior inferior iliac spine
3.0 mm	12 o'clock on acetabular rim
4.0 mm	Indirect head of the rectus femoris tendon center

For each phase of the suction seal test, the joint was reduced and manually distracted to determine whether a suction seal was present. As described by Suppauksorn et al,[39,40] the potted acetabulum and femur were then placed in neutral position in the tensile testing system for quantitative analysis, articulating with one another (Figure 3A). To create a suction seal, we initially applied a 250-N compressive load across the joint and subsequently distracted it at a rate of 10 mm/s until the suction seal was broken.[39,40] Load, time, and crosshead displacement were continuously recorded at 48 Hz. Both manually and during testing, the presence of a suction seal was confirmed with an audible "popping sound" produced as the seal was broken.

Contact pressure testing was performed using a dynamic contact pressure and area mapping system with thin-film load sensors (Model 5101; Tekscan Inc) placed within the hip joint. The specimens were positioned with an acetabular inclination of 40° in the horizontal plane and a pubic-femoral neck angle of 140° in the axial plane. The pressure sensors were each calibrated by a 2-point loading method within a separate customized jig per the manufacturer's specifications. For testing, a load of 700 N was applied to the joint (simulating approximately three-quarters of the mean body weight), and the specimens were tested with the femurs in neutral flexion and extension and in 20° of extension and 60° of flexion, with neutral internal-external rotation and adduction-abduction in both conditions as previously performed in a similar investigation.[19] Each of these 3 positions was tested 3 times. The primary outcomes, including contact area, contact pressure, and peak force, were averaged over the 3 trials. After testing the specimens in the intact state, we reproduced the same protocols for tests after the creation of a labral tear using a scalpel blade at the chondrolabral junction between 3 and 12 o'clock, corresponding to the location where most labral tears occur.[35]

The next 2 test groups consisted of a reconstructed labrum with both the ITB, harvested from the same specimen, and the IHRF. All aspects of the labral reconstruction were performed by a single, fellowship-trained surgeon (S.G.). The ITB graft was tubularized with the use of 2-0 absorbable sutures (Vicryl; Ethicon Inc) to produce a graft similar in geometry to the native labrum.[19] On the other

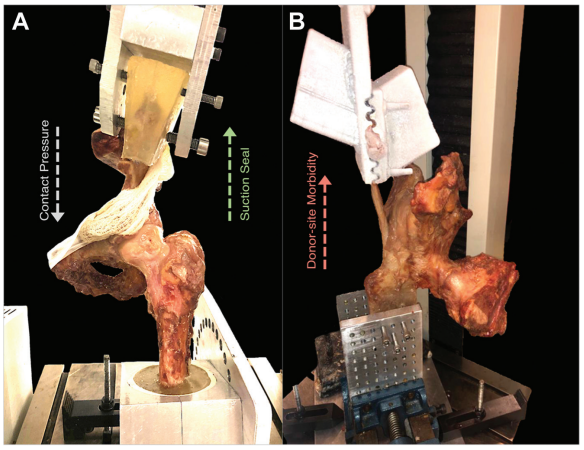

Figure 3. Mechanical testing setups with specific positioning of the cadaveric specimen using customized mounts. (A) Neutral position of a left hemipelvis during suction seal testing and contact pressure testing. In addition to this, neutral position contact pressure was tested with the femurs in both neutral flexion and extension and in 20° of extension and 60° of flexion, with neutral internal-external rotation and adduction-abduction in each testing state. (B) Inverted position of a left hemipelvis during the donor-site morbidity testing with the rectus femoris muscle belly held in a custom cryoclamp attached to the test machine actuator.

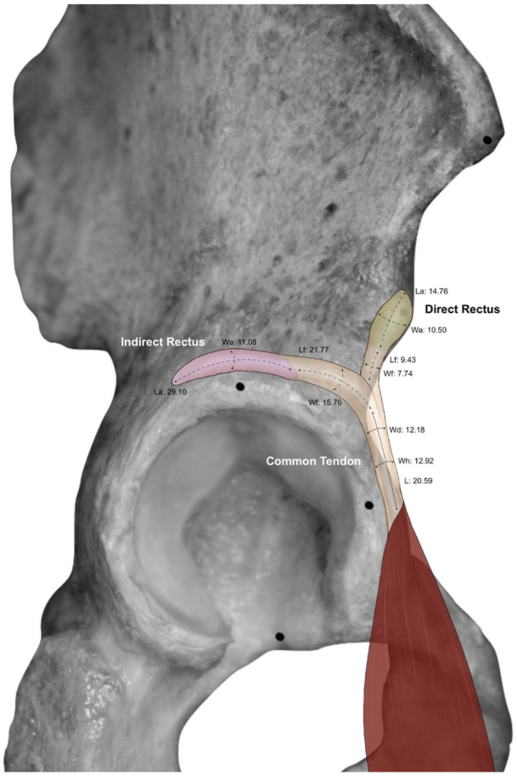

Figure 4. Gross anatomic specimen with artistic representation of the direct and indirect attachments of the rectus femoris tendon with mean caliper measurements. *a*, attached; *d*, distal; *f*, free; *h*, half; *L*, length; *W*, width.

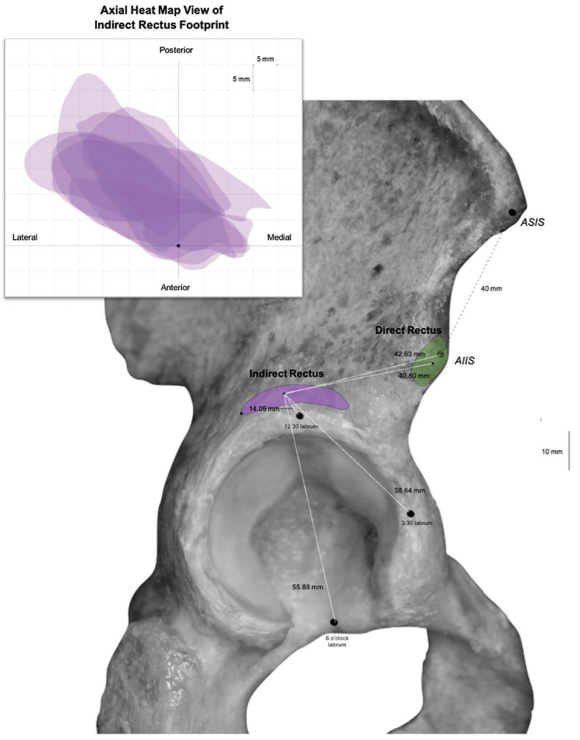

Figure 5. Gross anatomic figure with an artistic representation of indirect and direct head of the rectus femoris footprints as well as mean distances of the IHRF footprint centroid to local landmarks: anterior inferior iliac spine (AIIS), direct footprint centroid, 12:30 labral position, 3:30 labral position, and 6-o'clock labral position. All distances were derived from the 3D Microscribe system. The coordinates of the rectus femoris footprint perimeter from each specimen were overlaid to generate the heatmap in a top-down view, standardized to the 12:30 labral position. ASIS, anterior superior iliac spine.

hand, there was no need for tubularization of the IHRF graft, which was harvested by splitting the distal third of the tendon width in parallel to the longitudinal fibers.[37] The first graft was secured to the labral base of the resected segment with 3 double-loaded suture anchors (2.3 mm ICONIX; Stryker); evenly spaced on the acetabular rim, with care taken to avoid penetration of the acetabular articular surface; and finished with a looped suture configuration. After testing with the first graft was completed, the graft was released from the anchors by cutting the suture and keeping the anchors intact. The second graft was then secured in place with a second suture threaded through the anchors and tested in the same manner.

Finally, for assessment of potential morbidity after graft harvesting from the IHRF, each full pelvis had both IHRF tendons (intact vs contralateral IHRF with the harvested section removed) tested in tension along their anatomic fibers to compare differences between the intact specimens and the specimens with a harvested tendon. For testing, each hemipelvis was secured into custom jigs in an inverted position, with the rectus femoris muscle belly held in a custom cryoclamp attached to the test machine

actuator (Figure 3B). The mounted rectus femoris muscle was then pulled in line with the femoral axis. The test procedure involved preconditioning with a 10-N load applied to the construct for 2 minutes, cyclic testing from 50 to 200 N for 100 cycles, and then pull-to-failure testing at 1 mm/s until failure. Outcome measures including cyclic creep, the amount of construct elongation at the end of the test, and elongation amplitude, the amount the last cycle must travel between the upper and lower load limits, were calculated. From the failure tests, maximal load, construct stiffness (calculated from the linear portion of the load over the displacement curve), and failure mode were also determined. Failure modes were defined as tendon failure, bony avulsion, tendon slip from the grip, or bone failure in the grip and recorded. Intact and harvested tendons were tested in randomized order.

Statistical Analysis

Statistical analysis was performed in Stata Version 16.1 (StataCorp) and R (Version 4.1.0; R Foundation for Statistical Computing). To determine interrater reliability and precision in measurements, we calculated intraclass correlation coefficients for gross anatomic caliper measurements using a 2-way random-effects model. For the pressure mapping study, measurements were performed 3 times for each state, and the mean value was used for analysis. These values were normalized with respect to the intact specimen during the contact pressure testing analysis to account for variations in contact maps due to specimen size and cartilage wear, and both raw and adjusted data are presented. For suction seal analysis, the mean peak load values were adjusted with respect to no suction seal values during the suction seal analysis to remove any load output due to bony anomaly during testing. Those values were then normalized with respect to intact values from each specimen to account for each hip's inherent differences in intact suction seal. Nonparametric tests were used for comparison of groups to enable statistical comparisons independent of normality assumptions. Friedman test was performed to evaluate differences in biomechanical parameters between the conditions. Post hoc pairwise Wilcoxon rank-sum test with Bonferroni correction was used for multiple comparisons when significant differences were noted. Wilcoxon rank-sum test was used to compare cyclic testing and pull-to-failure testing between intact and harvested IHFR groups. All testing was 2-sided, and the level of significance was set at $P < .05$.

RESULTS

Gross Anatomic Measurements

Anatomic measurements of the common, IHRF, and direct head of the rectus femoris tendons taken via a digital caliper are depicted within Figure 4 (full measurements in Appendix Table A1, available in the online version of this article). The common rectus femoris tendon length was 20.6 ± 6.1 mm, with widths of 12.9 ± 2.1 mm and 12.2 ± 1.9 mm at the half and distal portions of the tendon, respectively. The width of the common tendon at the bifurcation was 20.2 ± 3.0 mm. Additionally, the tendon thicknesses were 7.6 ± 1.4 mm and 6.8 ± 1.2 mm at the half and distal portions of the tendon, respectively.

The lengths of the direct head of the rectus femoris were 9.4 ± 2.6 mm and 14.8 ± 3.3 mm at the free and attached portions, respectively. The widths of the direct head were 7.7 ± 2.0 mm proximal to the attachment and 10.5 ± 2.4 mm at the attachment. The lengths of the indirect head at the free and attached portions of the rectus femoris were 21.8 ± 5.2 mm and 29.1 ± 7.2 mm, respectively. The widths of the IHRF tendon were 11.1 ± 1.7 mm at and 15.8 ± 2.4 mm proximal to the attachment.

Three-Dimensional Anatomy

The surface area measurements of the direct and IHRF tendon footprints were calculated to be 111.2 ± 40.0 mm^2 and 85.1 ± 26.8 mm^2, respectively. Calculated distances in the sagittal, axial, and coronal planes, as well as the total 3D distances, are depicted in Figure 5 (full measurements in Appendix Table A2, available online). The centroid of the IHRF attachment was located 10.3 ± 2.6 mm posterior, 2.5 ± 7.8 mm superior, and 5.0 ± 2.8 mm lateral to the 12:30 labral position. The posterior apex of the IHRF attachment was located 21.0 ± 6.5 mm posterior, 0.7 ± 8.0 mm superior, and 22.2 ± 4.4 mm lateral to the 12:30 labral position.

Radiographic Anatomy

In radiographic analysis of the full pelvis specimens, the mean distance of the IHRF to the following landmarks was measured: anterior inferior iliac spine (8.8 ± 2.5 mm), direct head of the rectus femoris (8.0 ± 3.9 mm), 12-o'clock labral position (14.1 ± 2.8 mm), and 3-o'clock labral position (36.5 ± 4.4 mm) (Figure 6).

Biomechanical Assessment

Suction Seal. Of 8 specimens undergoing manual suction seal testing, 1 specimen failed to demonstrate a suction seal in the intact state and therefore was excluded from testing. During testing, 1 additional specimen was excluded due to a technical preparation failure. Therefore, 6 specimens were included in the final analysis.

Among all 6 fully tested specimens, both the ITB and rectus femoris reconstruction groups demonstrated a negative manual suction seal test—defined as an absent suction seal—while the intact and tear groups demonstrated a positive manual suction seal test. This was tested by applying a manual distracting force across the hip joint until confirmation of the suction seal. Load-displacement curves demonstrating the measured force for each group are shown in a representative graph of results from 1 specimen (Figure 7). Because of the negative manual seal test in the reconstruction groups, the measured peak force within the reconstruction groups was determined to be attributed to bony impingement on the acetabulum. This is because

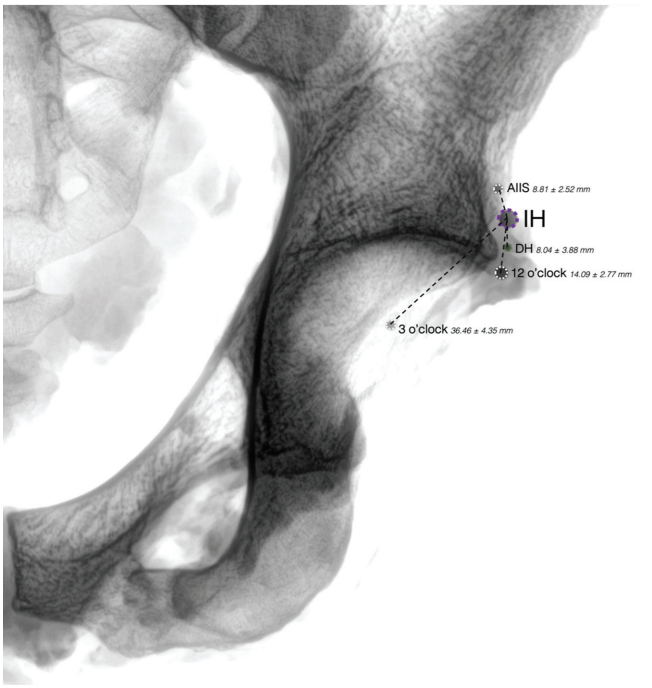

Figure 6. Anteroposterior view of pelvis specimen with radiographic markers highlighting the indirect rectus femoris head (IH), direct rectus femoris head (DH), anterior inferior iliac spine (AIIS), and 12- and 3-o'clock labral positions. The radiographic distances between the IH and 4 landmarks are demonstrated as mean ± SD.

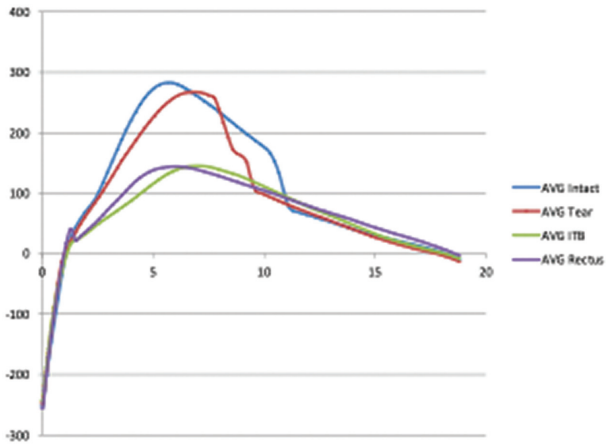

Figure 7. Sample load-displacement curves for comparison of suction seal effects between groups in 1 representative specimen. Because the reconstruction groups demonstrated no manual suction seals, the measured peak can be attributed to bony impingement from the acetabulum caused by the direction of loading. Therefore, the mean peak load values of the reconstruction groups were used to determine the approximate effect of bony impingement and adjust all values accordingly. AVG, average; ITB, iliotibial band.

the direction of pulled force was axial, versus a pure distraction force across the hip joint in line with the femoral neck. With axial pull, there was impingement between the femoral head and inferior acetabulum. Therefore, peak load and energy to peak load values for all groups were adjusted per specimen to account for bony impingement (Appendix Table A3, available online). In addition, to account for differences in intact suction seal measurements between specimens, data were normalized with respect to each specimen's intact state.

Comparing both adjusted and unadjusted normalized data, we demonstrated significant differences between groups in measured peak loads and energy to peak loads ($P = .002$). Both the ITB and the rectus femoris reconstruction groups had significantly lower peak loads and lower energy to peak loads compared with both intact and tear groups ($P = .013$ to $.017$ for all comparisons). There were no significant differences between the reconstruction groups for any outcome or between any groups for displacement at peak load (Figure 8).

Joint Contact Area, Contact Pressure, and Peak Force. All 8 hemipelvis specimens successfully completed contact pressure mapping and were included for analysis (Appendix Table A4, available online). A schematic montage of all 4 states and 3 joint positions from 1 representative specimen is shown in Figure 9. Quantitative data from pressure mapping were normalized with respect to each specimen's intact values per joint position.

In the neutral position, there were significant differences between groups in normalized contact area ($P = .01$) and normalized contact pressure ($P = .007$) (Figure 10). Relative to the intact group, the ITB reconstruction group had a significantly lower contact area (100% vs 57.5%; $P = .003$), while the rectus femoris reconstruction group had a similar contact area (100% vs 61.0%; $P = .050$). As a result, the ITB reconstruction group had greater contact pressures compared with the intact group (100% vs 128.1%; $P = .003$), whereas the rectus femoris reconstruction group had similar contact pressures (100% vs 130.2%; $P = .050$, respectively).

In 20° of extension, there were significant differences in normalized contact area demonstrated among the groups ($P = .029$). On post hoc analysis, the ITB reconstruction group was found to have a similar contact area relative to the intact state (100% vs 67.7%; $P = .050$). There were no significant differences between the rectus femoris reconstruction group and the intact and tear groups ($P > .99$) or between the rectus femoris and ITB reconstruction groups ($P = .30$). In 60° of flexion, both normalized contact pressure and area demonstrated significant differences among groups ($P = .029$). On post hoc analysis, the ITB reconstruction group alone demonstrated a similar contact pressure (100% vs 144.8%; $P = .050$) and contact area (100% vs 65.6%; $P = .050$) relative to the intact state. There were no differences between the ITB and rectus femoris reconstruction groups ($P > .99$) nor any differences in the tear group in comparison with the other groups. Finally, no significant differences were observed in peak contact force between all groups in neutral ($P = .31$), flexion ($P = .58$), and extension ($P = .09$).

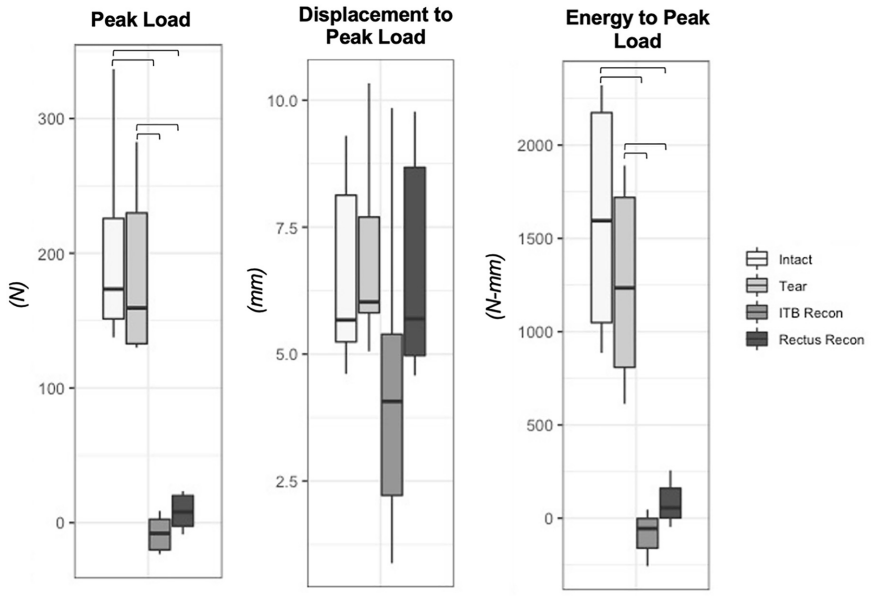

Figure 8. Box plots of adjusted values for peak force (load), displacement at peak load, and energy to peak load between groups. The iliotibial band (ITB) and rectus femoris reconstruction groups were not significantly different in peak load and energy to peak load (P = .39 to >.99). Both reconstruction groups demonstrated significantly lower peak load and energy to peak loads (P = .013 to .017) compared with intact and tear groups. No significant differences were detected among all groups for displacement to peak load. Recon, reconstruction.

Donor-Site Morbidity. Donor-site morbidity testing was performed on 8 full pelvis specimens, which were separated for testing, where contralateral pairs were assigned to intact or harvested specimens (Table 2). One intact hemipelvis was excluded because of an error during specimen preparation, leaving 8 harvested rectus femoris specimens and 7 intact rectus femoris specimens for analysis. All remaining specimens survived the cyclic test regimen. After grouping the data into intact and harvested groups, we found no significant differences between intact and harvested specimen measurements for cyclic creep (4.6 ± 1.8 vs 4.7 ± 2.5, respectively; P = .85) and elongation amplitude (1.9 ± 0.5 vs 1.9 ± 0.4, respectively; P = .65).

During failure testing, 2 specimens with harvested rectus femoris tendons were excluded from the analysis for technical failures involving tendon slip from the grip and poor fixation in the bone grip. Therefore, 6 harvested specimens and 7 intact specimens were included in the final failure analysis. Failure modes (No. intact/No. harvested) included tendon failure (3/3), bone failure in grip (3/3), and bony avulsion (1/0). There were no significant differences in maximal load to failure (intact vs harvested: 1529.7 ± 507.7 vs 1425.9 ± 389.4; P = .78), construct stiffness (118.2 ± 55.6 vs 105.3 ± 24.8; P = .89), or failure mode (P = .63) between the 2 groups.

DISCUSSION

The main findings of the study were as follows: (1) The IHRF tendon is adjacent to the acetabulum and has suitable length for segmental labral reconstruction. A 2-cm graft can be harvested from the "free" nonattached portion of the tendon. (2) Although inferior to intact labra, rectus femoris tendon graft labral reconstruction exhibits biomechanical properties similar to those of ITB reconstruction. (3) Rectus femoris tendon graft harvest does not cause donor-site morbidity in the remaining tendon. These findings in conjunction confirm our hypothesis and confirm the viability of the IHRF graft in segmental labral reconstruction.

The posterior apex of the IHRF attachment, which is the starting point for graft harvesting, was shown to be in close proximity to the labrum. Consequently, the IHRF is a reasonable local autograft option and is adequately sized in length and thickness for use during segmental labral reconstruction, but it is not appropriate for circumferential reconstruction. This is because the demonstrated length of the IHRF can cover the length between the 12- and 3-o'clock positions[15] but not the full circumference of the labrum.[21] Nonetheless, ideal graft options and sources for reconstructing the labrum are still widely debated in the literature.[23] A recent study by Maldonado et al[22] compared clinical outcomes of 17 patients who underwent primary labral reconstruction with a hamstring allograft with those of 12 patients with autograft after 2 years of follow-up and found no differences between the groups. Despite the inherent advantages of allografts, such as decreased surgical time and avoidance of donor-site morbidity, some of their disadvantages must also be noted. Reasons for many surgeons preferring autografts include potential disease transmission, delayed incorporation, increased costs, and patient refusal of allografts.[4,14,23,32,36] Furthermore, because the IHRF tendon is anatomically close to the

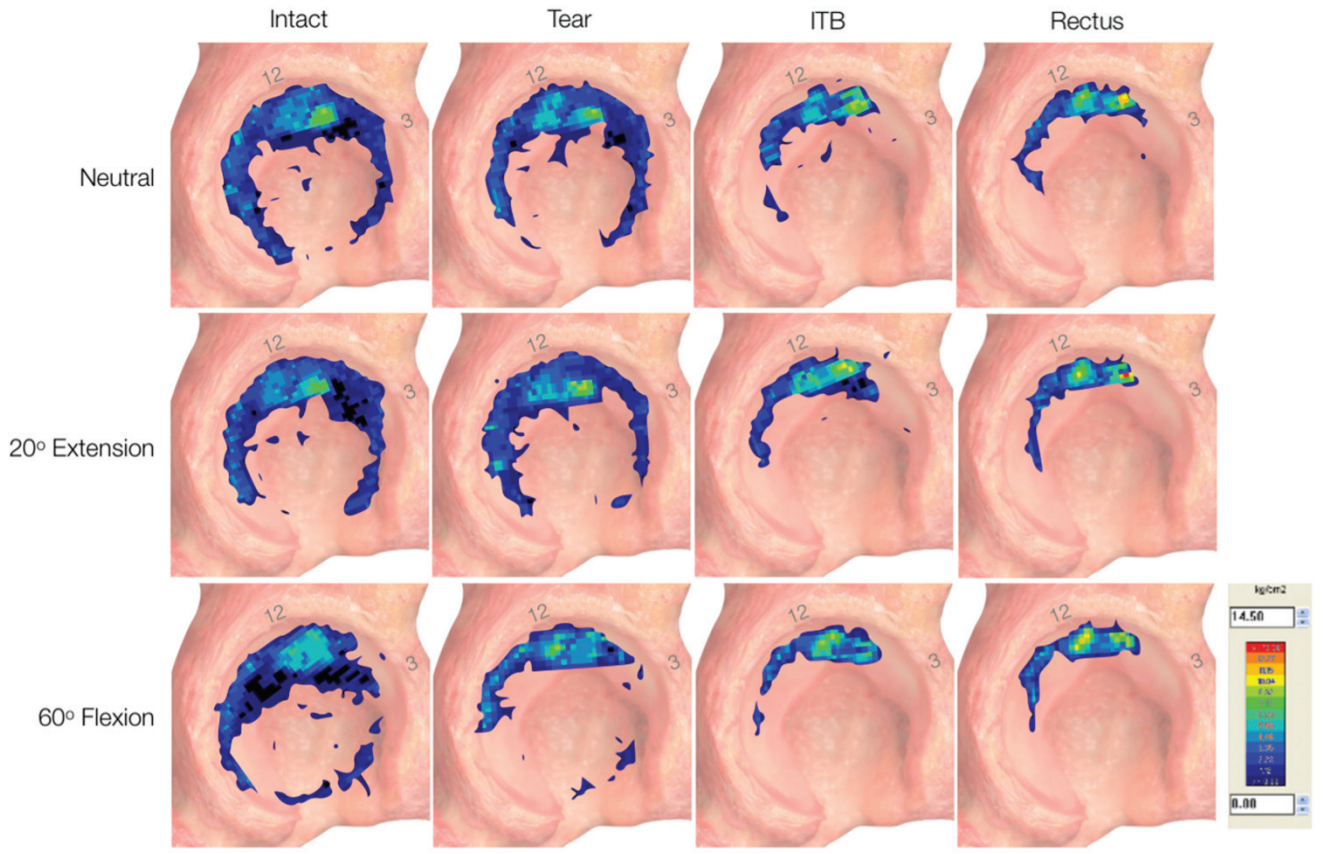

Figure 9. Anatomic figure overlaid with real-time pressure and area map measurements of a representative right hip acquired using I-Scan software (Version 5.83; Tekscan). Blue indicates low pressure, while yellow and orange indicate higher pressure. ITB, iliotibial band.

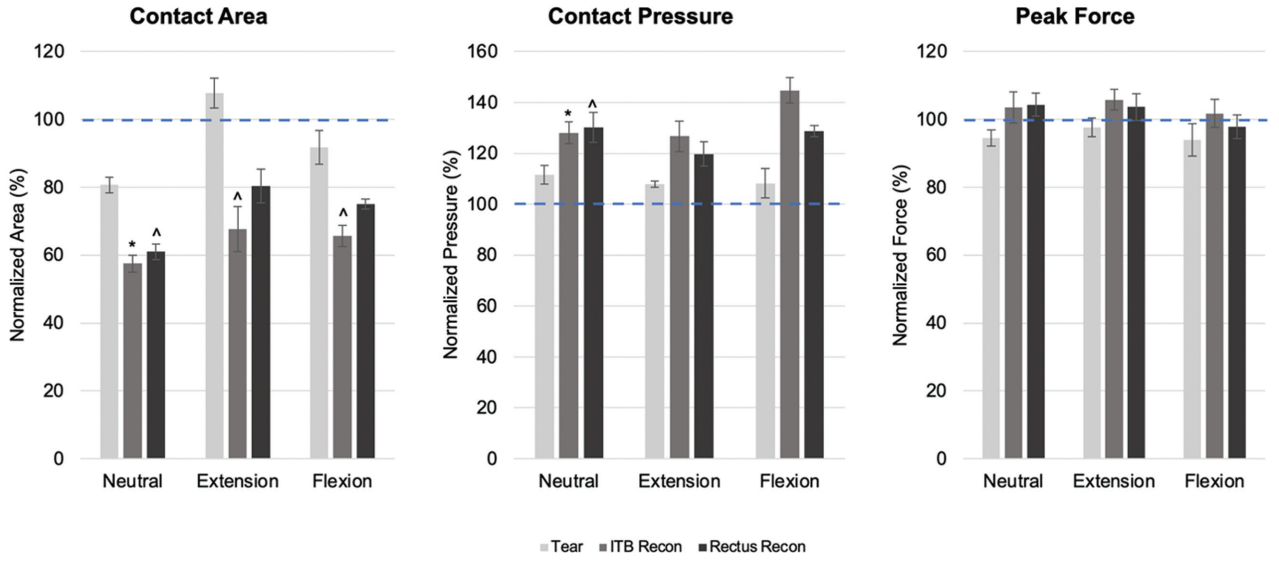

Figure 10. Contact pressure measurements normalized to intact values. Dotted line indicates intact group (100%). Statistical comparisons to intact: *$P < .05$; ^$P = .05$. ITB, iliotibial band; Recon, reconstruction.

TABLE 2
Morbidity Testing of Cadaveric Specimens After Rectus Femoris Graft Harvesting[a]

	Rectus Femoris Intact	Rectus Femoris Harvested	*P*
Cyclic testing	n = 7	n = 8	
Cyclic creep, mm	4.6 ± 1.8	4.7 ± 2.5	.85
Elongation amplitude, mm	1.9 ± 0.5	1.9 ± 0.4	.65
Failure testing	n = 7	n = 6	
Mode of failure (n)	Tendon failure (3), bony avulsion (1), bone failure in grip (3)	Tendon failure (3), bone failure in grip (3)	.63
Maximal load, N	1529.7 ± 507.7	1425.9 ± 389.4	.78
Stiffness, N/mm	118.2 ± 55.6	105.3 ± 24.8	.89

[a]Data are presented as mean ± SD unless otherwise indicated.

acetabular rim, an additional advantage of the rectus femoris graft is that harvesting does not require an additional portal or incision. The location of the centroid of the IHRF tendon was calculated to be in close proximity to the 12:30 labral position. In the setting of a large pincer deformity where it is difficult to gain proper traction, it is preferred to access the joint in an outside-in fashion to avoid damaging the labrum or femoral head cartilage.[28] The measurements provided in the current study on the IHRF can be used to guide an outside-in approach during anatomic localization of the intraportal capsulotomy 1 cm distal to the labrum with no additional portal created. Ultimately, these findings corroborate previous anatomic descriptions found in the literature regarding the IHRF tendon[2,13,30] and are reinforced by radiological evidence presented in this study. However, unlike previous studies, this investigation provides data on not only the native location of the tendon attachment site but also relative distances with surrounding landmarks that would directly facilitate arthroscopic orientation, serving as a guide for harvesting the IHRF tendon. Additionally, the failure analysis focused on final failure load but did not measure yield load, which would also be of clinical interest as the point of plastic deformation. During hip arthroscopy, fluoroscopy is useful because of the complex 3D anatomy of the hip joint. Fluoroscopic guidance is used in many stages, from placing the portals to determining the localization of bone deformities and confirming an appropriate amount of resection.[17] Intraoperative fluoroscopy for evaluation of bony resection during arthroscopic management of femoroacetabular impingement is accomplished in the supine position.[17] The radiological data provided by the current study regarding the attachment of the IHRF tendon may facilitate intraoperative orientation during autograft harvesting.

In the current study, the dimensions of the IHRF tendon were described, allowing for proper application based on the type of reconstruction. Labral reconstruction techniques can be segmental or circumferential. Circumferential reconstruction is preferred in advanced diffuse labral degeneration or cases requiring a comprehensive pincer-type impingement correction.[9] During this reconstruction, it is recommended to prepare a graft with an 85- to 145-mm length and 5- to 6-mm diameter.[21] Although graft length is intraoperatively determined and validated based on the area of the segmental defects, Karns et al[15] conducted an anatomic study reporting that acetabular tears were more frequently encountered within the distance between the 12- and 3-o'clock positions of the acetabulum. This length was measured to be approximately 4.88 cm in male and 4.32 cm in female cadaveric specimens. In the same study, the 270° circumferential rim lengths of the acetabulum were found to be 15.82 cm and 13.67 cm in male and female specimens, respectively. Given the dimensions of the IHRF tendon measured in the current study, the rectus femoris graft may not be appropriate for a circumferential reconstruction or large segmental reconstruction because it would not provide a sufficient graft length even when the common tendon is included in graft harvesting. On the other hand, a sufficient graft length can be obtained for segmental reconstruction. Insufficient length of the IHRF tendon for circumferential labral reconstruction may explain why it is not the most commonly preferred option during labral reconstruction.

A particular concern regarding the use of autografts in treating musculoskeletal pathologies is the potential donor-site morbidity caused by graft harvesting.[6,26,42] In clinical studies, authors have postulated that because the graft is locally available and does not require any additional incision or portal to harvest, employing the IHRF tendon as a graft in labral reconstruction inherently negates any risk of donor-site morbidity.[20,33] The biomechanical results from the current investigation are no exception, demonstrating no significant differences between specimens with an intact and harvested IHRF during cyclic and pull-to-failure testing, thereby affirming that harvesting the IHRF tendon does not lead to donor-site morbidity. As such, the data presented in this study appear to be consistent with published peer-reviewed literature and support our hypothesis of IHRF viability as a local autograft.

Given its proximity to the anterolateral portal in addition to strong evidence of excellent clinical and biomechanical outcomes,[5,19,21] the ITB is widely used as the preferred graft choice for many surgeons. Despite this preference, the current study detected no significant differences between labral reconstruction performed using the IHRF tendon and ITB with respect to contact area, contact pressure, and peak force. Although there are no investigations directly comparing the 2 graft options, the ITB graft has been frequently studied from both clinical and biomechanical

perspectives.[5,19,21] Geyer et al[12] published one of the largest case series on labral reconstruction using iliotibial autografts in 75 patients, reporting significant improvements in the modified Harris Hip Score of about 24 points as well as in the Hip Outcome Score Sports and Activities of Daily Living subscales. Similarly, Nakashima et al[27] used ITB grafts in 25 hips and reported that the mean modified Harris Hip Score exhibited a significant improvement from 67 points preoperatively to 95 points postoperatively at >2 years of follow-up, in addition to significant improvement in the mean Nonarthritic Hip Score. Biomechanically, studies have demonstrated significant improvements in the contact area, contact pressure, and peak force parameters in anterosuperior segmental labral reconstruction while replicating the tensile properties and geometry of the native labrum.[11,19] On the other hand, only a few small case series employing the IHRF tendon as an autograft in labral reconstruction have been published with comparable clinical outcomes reported.[1,20,33] However, to the best of our knowledge, there are no previous studies evaluating the biomechanics of the IHRF tendon in a labral reconstruction. Based on the cadaveric data obtained in the present study, the IHRF tendon possesses similar biomechanical properties to the ITB. Therefore, surgeons should consider the potential benefits of the IHRF for its strong basic science properties and advantages in surgical application.

This study is not without limitations. First, the labral tear was created and the reconstruction was performed using an open approach given the inability to conduct contact pressure testing without removing soft tissues. This could have led to different intra-articular contact pressures that would be obtained during arthroscopy and therefore may limit the generalizability of these findings to this surgical application. Because of the lack of similar biomechanical studies in the literature to establish an effect size and perform a priori power analysis, the present study may involve a potential risk of type 2 error, particularly in the results from the morbidity tests. Another limitation of the study was the repeated use of cadavers for each testing state. Despite lubrication of the cartilage and labral surfaces with normal saline and cadaveric fat, it is possible to encounter cartilage compression and labral softening after performing repeated tests on the cadaveric hips. Therefore, this may have affected some of the changes in contact pressure measured. Moreover, repeated tests may have also broken the suction seal. To control for this, the order of ITB and rectus femoris labral reconstruction was randomized. Third, the tissue quality became poorer due to ranked repeated tests, and this may have led to a higher incidence of failure during the morbidity tests, as they were performed last. The suction seal was assessed using the testing model defined by Suppauksorn et al.[39,40] For repetitive tests in this model, the ligamentum teres was sectioned, and saline bath was not used, unlike in some previous studies in the literature. The fact that this situation does not reproduce native conditions sufficiently can be considered another limitation of the study. Finally, although the tests performed in the study were carried out at different positions of the hip to simulate the normal arc of motion of the hip, the cadaveric model only shows the contact pressure at time zero.

CONCLUSION

The IHRF tendon is within close anatomic proximity to arthroscopic acetabular orientations and possesses sufficient thickness and length for segmental labral reconstruction. In this cadaveric model, harvesting of the IHRF tendon as an autograft did not lead to significant donor-site morbidity in the remaining tendon. Segmental labral reconstruction performed with the IHRF tendon exhibited similar biomechanical outcomes compared with that performed with the ITB.

ORCID iD

Amar S. Vadhera https://orcid.org/0000-0001-5225-4641

REFERENCES

1. Amar E, Sampson TG, Sharfman ZT, et al. Acetabular labral reconstruction using the indirect head of the rectus femoris tendon significantly improves patient reported outcomes. *Knee Surg Sports Traumatol Arthrosc*. 2018;26(8):2512-2518.
2. Atzmon R, Sharfman ZT, Atoun E, et al. The anatomical properties of the indirect head of the rectus femoris tendon: a cadaveric study with clinical significance for labral reconstruction surgery. *Arch Orthop Trauma Surg*. 2020;140(1):85-92.
3. Bachmann G, Basad E, Lommel D, Steinmeyer J. MRI in the follow-up of matrix-supported autologous chondrocyte transplantation (MACI) and microfracture. Article in German. *Radiologe*. 2004;44(8):773-782.
4. Barbour SA, King W. The safe and effective use of allograft tissue—an update. *Am J Sports Med*. 2003;31(5):791-797.
5. Bessa FS, Williams BT, Polce EM, et al. Indications and outcomes for arthroscopic hip labral reconstruction with autografts: a systematic review. *Front Surg*. 2020;7:61.
6. Bexkens R, Ogink PT, Doornberg JN, et al. Donor-site morbidity after osteochondral autologous transplantation for osteochondritis dissecans of the capitellum: a systematic review and meta-analysis. *Knee Surg Sports Traumatol Arthrosc*. 2017;25(7):2237-2246.
7. Chandrasekaran S, Darwish N, Close MR, et al. Arthroscopic reconstruction of segmental defects of the hip labrum: results in 22 patients with mean 2-year follow-up. *Arthroscopy*. 2017;33(9):1685-1693.
8. Domb BG, El Bitar YF, Stake CE, et al. Arthroscopic labral reconstruction is superior to segmental resection for irreparable labral tears in the hip: a matched-pair controlled study with minimum 2-year follow-up. *Am J Sports Med*. 2014;42(1):122-130.
9. Domb BG, Kyin C, Rosinsky PJ, et al. Circumferential labral reconstruction for irreparable labral tears in the primary setting: minimum 2-year outcomes with a nested matched-pair labral repair control group. *Arthroscopy*. 2020;36(10):2583-2597.
10. Ferguson SJ, Bryant JT, Ganz R, Ito K. An in vitro investigation of the acetabular labral seal in hip joint mechanics. *J Biomech*. 2003;36(2):171-178.
11. Ferro FP, Philippon MJ, Rasmussen MT, et al. Tensile properties of the human acetabular labrum and hip labral reconstruction grafts. *Am J Sports Med*. 2015;43(5):1222-1227.
12. Geyer MR, Philippon MJ, Fagrelius TS, Briggs KK. Acetabular labral reconstruction with an iliotibial band autograft: outcome and survivorship analysis at minimum 3-year follow-up. *Am J Sports Med*. 2013;41(8):1750-1756.

13. Hapa O, Bedi A, Gursan O, et al. Anatomic footprint of the direct head of the rectus femoris origin: cadaveric study and clinical series of hips after arthroscopic anterior inferior iliac spine/subspine decompression. *Arthroscopy*. 2013;29(12):1932-1940.
14. Kainer MA, Linden JV, Whaley DN, et al. Clostridium infections associated with musculoskeletal-tissue allografts. *N Engl J Med*. 2004;350(25):2564-2571.
15. Karns MR, Patel SH, Kolaczko J, et al. Acetabular rim length: an anatomical study to determine reasonable graft sizes for labral reconstruction. *J Hip Preserv Surg*. 2017;4(1):106-112.
16. Larson CM, Giveans MR, Stone RM. Arthroscopic debridement versus refixation of the acetabular labrum associated with femoroacetabular impingement: mean 3.5-year follow-up. *Am J Sports Med*. 2012;40(5):1015-1021.
17. Larson CM, Wulf CA. Intraoperative fluoroscopy for evaluation of bony resection during arthroscopic management of femoroacetabular impingement in the supine position. *Arthroscopy*. 2009;25(10): 1183-1192.
18. Lebus GF, Briggs KK, Dornan GJ, McNamara S, Philippon MJ. Acetabular labral reconstruction: development of a tool to predict outcomes. *Am J Sports Med*. 2018;46(13):3119-3126.
19. Lee S, Wuerz TH, Shewman E, et al. Labral reconstruction with iliotibial band autografts and semitendinosus allografts improves hip joint contact area and contact pressure: an in vitro analysis. *Am J Sports Med*. 2015;43(1):98-104.
20. Locks R, Chahla J, Bolia IK, Briggs KK, Philippon MJ. Outcomes following arthroscopic hip segmental labral reconstruction using autologous capsule tissue or indirect head of the rectus femoris tendon. *J Hip Preserv Surg*. 2018;5(1):73-77.
21. Lodhia P, McConkey MO, Leith JM, et al. Graft options in hip labral reconstruction. *Curr Rev Musculoskelet Med*. 2021;14(1):16-26.
22. Maldonado DR, Lall AC, Laseter JR, et al. Primary hip arthroscopic surgery with labral reconstruction: is there a difference between an autograft and allograft? *Orthop J Sports Med*. 2019;7(3):2325967 119833715.
23. Maldonado DR, Lall AC, Walker-Santiago R, et al. Hip labral reconstruction: consensus study on indications, graft type and technique among high-volume surgeons. *J Hip Preserv Surg*. 2019;6(1):41-49.
24. Martin-Carreras T, Sebro R, Weintraub S. Hip alpha angle is associated with anterior-superior labral tears but not anterior labral tears. *Curr Probl Diagn Radiol*. 2021;50(2):159-163.
25. Matsuda DK, Burchette RJ. Arthroscopic hip labral reconstruction with a gracilis autograft versus labral refixation: 2-year minimum outcomes. *Am J Sports Med*. 2013;41(5):980-987.
26. Mouarbes D, Menetrey J, Marot V, et al. Anterior cruciate ligament reconstruction: a systematic review and meta-analysis of outcomes for quadriceps tendon autograft versus bone–patellar tendon–bone and hamstring-tendon autografts. *Am J Sports Med*. 2019;47(14): 3531-3540.
27. Nakashima H, Tsukamoto M, Ohnishi Y, et al. Clinical and radiographic predictors for unsalvageable labral tear at the time of initial hip arthroscopic management for femoroacetabular impingement. *Am J Sports Med*. 2019;47(9):2029-2037.
28. Narvaez MV, Cady A, Serrano B, Youssefzadeh K, Banffy M. Outside-in capsulotomy of the hip for arthroscopic pincer resection. *Arthrosc Tech*. 2021;10(3):e615-e620.
29. Nepple JJ, Philippon MJ, Campbell KJ, et al. The hip fluid seal—part II: the effect of an acetabular labral tear, repair, resection, and reconstruction on hip stability to distraction. *Knee Surg Sports Traumatol Arthrosc*. 2014;22(4):730-736.
30. Philippon MJ, Michalski MP, Campbell KJ, et al. An anatomical study of the acetabulum with clinical applications to hip arthroscopy. *J Bone Joint Surg Am*. 2014;96(20):1673-1682.
31. Philippon MJ, Nepple JJ, Campbell KJ, et al. The hip fluid seal—part I: the effect of an acetabular labral tear, repair, resection, and reconstruction on hip fluid pressurization. *Knee Surg Sports Traumatol Arthrosc*. 2014;22(4):722-729.
32. Rahl MD, LaPorte C, Steinl GK, et al. Outcomes after arthroscopic hip labral reconstruction: a systematic review and meta-analysis. *Am J Sports Med*. 2020;48(7):1748-1755.
33. Rathi R, Mazek J. Arthroscopic acetabular labral reconstruction with rectus femoris tendon autograft: our experiences and early results. *J Orthop*. 2018;15(3):783-786.
34. Ross JR, Larson CM, Bedi A. Indications for hip arthroscopy. *Sports Health*. 2017;9(5):402-413.
35. Schmerl M, Pollard H, Hoskins W. Labral injuries of the hip: a review of diagnosis and management. *J Manipulative Physiol Ther*. 2005;28(8):632.
36. Schmidt-Hebbel A, Gomez C, Aviles C, et al. No association between positive intraoperative allograft cultures and infection rates after reconstructive knee ligament surgery. *Knee*. 2018;25(6):1129-1133.
37. Sharfman ZT, Amar E, Sampson T, Rath E. Arthroscopic labrum reconstruction in the hip using the indirect head of rectus femoris as a local graft: surgical technique. *Arthrosc Tech*. 2016;5(2):e361-e364.
38. Storaci HW, Utsunomiya H, Kemler BR, et al. The hip suction seal, part I: the role of acetabular labral height on hip distractive stability. *Am J Sports Med*. 2020;48(11):2726-2732.
39. Suppauksorn S, Beck EC, Chahla J, et al. Comparison of suction seal and contact pressures between 270 degrees labral reconstruction, labral repair, and the intact labrum. *Arthroscopy*. 2020;36(9):2433-2442.
40. Suppauksorn S, Parvaresh KC, Rasio J, Shewman EF, Nho SJ. The effect of rim preparation, labral augmentation, and labral reconstruction on the suction seal of the hip. *Arthroscopy*. 2022;38(2):365-373.
41. Utsunomiya H, Storaci HW, Rosenberg SI, et al. The hip suction seal, part II: the effect of rim trimming, chondrolabral junction separation, and labral repair/refixation on hip distractive stability. *Am J Sports Med*. 2020;48(11):2733-2739.
42. Valderrabano V, Leumann A, Rasch H, et al. Knee-to-ankle mosaicplasty for the treatment of osteochondral lesions of the ankle joint. *Am J Sports Med*. 2009;37(suppl 1):105S-111S.
43. Walker JA, Pagnotto M, Trousdale RT, Sierra RJ. Preliminary pain and function after labral reconstruction during femoroacetabular impingement surgery. *Clin Orthop Relat Res*. 2012;470(12):3414-3420.
44. Wu G, Siegler S, Allard P, et al. ISB recommendation on definitions of joint coordinate system of various joints for the reporting of human joint motion—part I: ankle, hip, and spine. *J Biomech*. 2002;35(4):543-548.

For reprints and permission queries, please visit Sage's Web site at http://www.sagepub.com/journals-permissions